# Development of a Control System for an Innovative Parallel Robot Used in Laparoscopic Pancreatic Surgery

Doina Pisla<sup>1,3</sup> a, Andra Ciocan<sup>1,2</sup> b, Bogdan Gherman<sup>1,\*</sup> c, Diana Schlanger<sup>2</sup> d, Alexandru Pusca<sup>1,\*</sup> e, Nadim Al Hajjar<sup>2</sup> f, Emil Mois<sup>2</sup> Andrei Cailean<sup>1</sup> Nicoleta Pop<sup>1</sup> paul Tucan<sup>1</sup> , Ionut Zima<sup>1</sup> and Calin Vaida<sup>1</sup>

<sup>1</sup>CESTER, Technical University of Cluj-Napoca, 400114 Cluj-Napoca, Romania

<sup>2</sup>Department of Surgery, "Iuliu Hatieganu" University of Medicine and Pharmacy, 400347 Cluj-Napoca, Romania

<sup>3</sup>Technical Sciences Academy of Romania, B-dul Dacia, 26, 030167 Bucharest, Romania

herman, Alexandru.Pusca, Andrei.Cailea, Po

dra.ciocan10@gmail.com, na hajjar@vahoo

Keywords: Parallel Robot, Master-Slave, Control System, Minimally Invasive Pancreatic Surgery, Robotic Assisted.

Abstract:

This paper presents the development of the control architecture for an innovative parallel robot, designed to assist surgeons during the minimally invasive pancreatic cancer surgery. Based on the defined medical protocol and surgeon requirements. The robot was designed to serve as a surgical assistant and to manipulate a third active instrument. The system features a 3-DOF parallel active module coupled to a passive spherical module guiding the instrument through a Remote Center of Motion (RCM). The master-slave control architecture enables surgeons to operate the robot using a 3D Space Mouse or haptic device (Omega.7). The system automatically calculates RCM position using IMU sensors, validated through optical tracking.

## 1 INTRODUCTION

Pancreatic cancer ranks 7th globally in terms of mortality rate and 14th in incidence. In Europe, it ranks 2<sup>nd</sup> in terms of the number of new cases, with countries such as Hungary, Slovakia, the Czech Republic, and Serbia reporting the highest rates (McGuigan, 2018) with a higher incidence in developed countries (Wong MCS, 2017). Risk factors include modifiable factors (obesity, diet, alcohol, smoking) and non-modifiable factors (age, gender, genetics) (McGuigan, 2018). The prognosis remains challenging with a 5-year survival rate of only 5%, increasing to 30% with early detection. However, early detections increase the 5-year survival rate to 30%. Treatment involves surgery combined with oncological therapy (Nortunen, 2023; Nießen, 2022). Three main surgical procedures are used for pancreatic cancer: Pancreaticoduodenectomy (Whipple Procedure) (Cawich, 2023), Distal Pancreatectomy (De Pastena, 2023), and Total Pancreatectomy (Balzano, 2023).

The first robotic-assisted distal pancreatectomy was performed using the da Vinci system in 2003 (Melvin, 2003), improving safety and feasibility compared to manual laparoscopic surgery leading to wider robotic surgery adoption (Damoli, 2015). Robotic systems (da Vinci, Senhance, Versius) offer advantages including the elimination of the triangulation effect, enhanced precision, improved dexterity, and increased patient safety, driving adoption in surgical interventions. These surgical robots reduce hand tremors, enable motion scaling and multi-instrument manipulation, improve ergonomics through master-slave control (Pisla, 2021), and support remote telesurgery interventions

alphttps://orcid.org/0000-0001-7014-9431

b https://orcid.org/0000-0003-0126-6428

<sup>&</sup>lt;sup>c</sup> https://orcid.org/0000-0002-4427-6231

dip https://orcid.org/0000-0002-4427-6231

https://orcid.org/0000-0002-5804-575X

fl https://orcid.org/0000-0001-5986-1233

glo https://orcid.org/0000-0002-2972-3777

https://orcid.org/0009-0004-4758-0468

https://orcid.org/0000-0001-5660-8259

https://orcid.org/0000-0001-5660-8259

k https://orcid.org/0009-0007-0483-7691

https://orcid.org/0000-0003-2822-9790

<sup>\*</sup> Corresponding author

(Li, 2023). Robotic-assisted surgery presents several disadvantages, including the high cost of surgical intervention, steep learning curves, potential arm collisions, significant space, the lack of haptic feedback, and the limited intraoperative space (Haidegger, 2022).

Most robots for laparoscopic surgery use masterslave architecture (Rus, 2023; Pisla, 2024 a). These robots operate without autonomy in minimally invasive surgery (Khachfe, 2022). These robotic systems lack haptic feedback for surgeons (Minamimura, 2024). Studies demonstrate haptic device integration in the Senhance robotic system (Kastelan, 2021). Force feedback sensors have been placed near the robot flange, but the research in this direction is in the early stages of development (Bergholz, 2023). Alternative control approaches using contactless interfaces have been explored. Korayem demonstrated Leap Motion controller integration for surgical robot control with Kalman filtering (Korayem, 2021), hand tremor detection and compensation techniques (Korayem, 2022 a), and complete laparoscopic robot system development (Korayem, 2022 b; Najafinejad, 2023).

Minimally invasive pancreatic procedures are complex, requiring multiple instruments, extended operative time, and involving high risks (Asbun, 2023), indicating significant research gaps in the field. To address these challenges, a new parallel robot was developed for minimally invasive pancreatic surgery (Vaida, 2025). The proposed robot acts as a surgical assistant during pancreatic laparoscopy, performing tissue manipulation tasks using an active surgical instrument.

The paper is structured as follows: Section 1 presents the introduction, section 2 outlines medical protocol, robot design and integration, and mathematical model implementation, section 3 illustrates the control architecture of the robot; section 4 illustrates the experimental testing and validation, while section 5 presents conclusions and future developments.

# 2 DESIGN OF THE INNOVATIVE SURGICAL PARALLEL ROBOT AND ACTIVE INSTRUMENT

The Athena parallel robot was developed based on a medical protocol (Figure 1) established in collaboration with surgeons. This protocol outlines the steps for laparoscopic pancreatic surgery targeting the head of the pancreas (Whipple Procedure).

Based on the medical protocol and surgeon's requirements, the kinematic scheme of the robot (Figure 2) was developed, together with an active instrument, both subject to two patents (Pisla, 2025 b; Vaida, 2025 a). The robot assists the main surgeon by manipulating a third active atraumatic instrument to create an intraoperative workspace and support organs around the pancreas. A detail of the tasks that the robot performs is extensively presented in (Vaida, 2025 b) and in (Tucan, 2025).

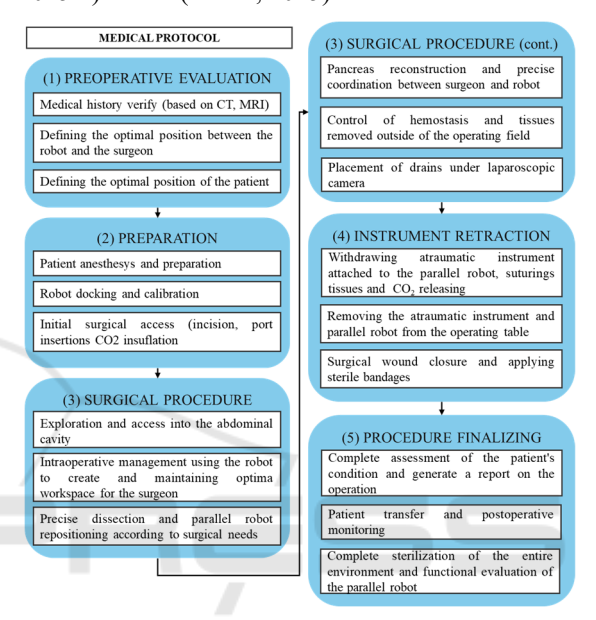


Figure 1: Medical protocol for laparoscopic pancreatic surgery.

The ATHENA parallel robot mechanical architecture (Figure 2) consists of two modules: an active 3 degrees-of-freedom (DOF) parallel robot and a passive parallel spherical mechanism. The spherical mechanism fixes and holds the Remote Center of Motion (Zhang, 2024), while the parallel robot manipulates the active surgical instrument. The robot consists of 9 passive revolute joints, three passive prismatic joints, three active prismatic joints (qi, i=1....3) and two passive universal joints. The global coordinate system is placed on the robot base. The spherical mechanism features five passive revolute joints and one passive cylindrical joint that provide rotation and insertion motion of the active instrument. The spherical mechanism connects to the robot base via a link and two spherical joints for RCM placement and adjustment.

Detailed description of parameters is presented in (Vaida, 2025), and integration of the robot into the medical environment is illustrated in Figure 3.

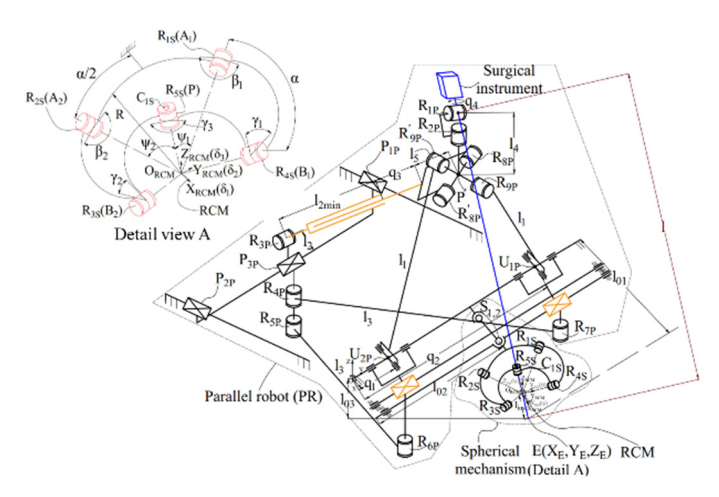


Figure 2: Kinematic scheme of the Athena robot.

Based on the kinematic scheme and parameters presented in (Vaida, 2025), kinematic models (forward and inverse) of the Athena robot were developed and integrated into the control system through input/output equations. Four mathematical models are used to control the robot: forward (Eqs. 2-5) and inverse (Eqs. 7-9) kinematic models without RCM, used for robot positioning near the patient and RCM before instrument attachment. Once the RCM is defined, the instrument is positioned at the abdominal insertion position and attached to the robot. In this configuration, inverse (Eqs. 5-6) and forward (Eqs. 7-9) kinematic models with RCM control both the robot and the surgical instrument.

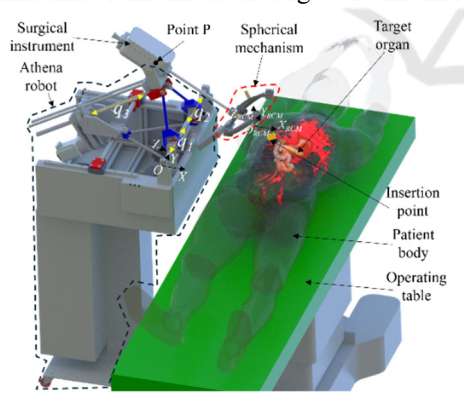


Figure 3: Athena robot integrated into the medical environment.

The equations for these models are:

$$f_{1}: l_{02} + (q_{1} + (q_{2} / 2)) - Y_{p} = 0$$

$$f_{2}: \left(l_{4} + \sqrt{l_{1}^{2} - (q_{2} - (q_{1} / 2))^{2}}\right)^{2} - (Z_{p} - l_{03})^{2} - (X_{p} - l_{01})^{2} = 0$$

$$f_{3}: (q_{3} + l_{2\min} + l_{5})^{2} - (X_{p} - l_{01} - l_{4} \cos(\lambda) + \sqrt{l_{3}^{2} - (q_{2} - (q_{1} / 2))^{2}}\right)^{2} - (Z_{p} - l_{4} \sin(\lambda) - l_{03})^{2} = 0$$
(1)

where:

$$\begin{split} X_{p} &= cos(\psi) sin(\theta)(l - l_{ins}); Y_{p} = sin(\psi) sin(\theta)(l - l_{ins}) \\ Z_{p} &= cos(\theta)(l - l_{ins}); \lambda = atan(Z_{p} - l_{03}, X_{p} - l_{01}). \end{split} \tag{2}$$

$$X_{p} = X_{p_{c}} + l_{4}cos(\beta); Y_{p} = Y_{p_{c}}; Z_{p} = Z_{p_{c}} + l_{4}sin(\beta)$$
(3)

and

$$\begin{split} X_{pc} &= -\sqrt{\left(l_{3}^{2} - \left(\left(q_{2} - q_{1}\right)/2\right)^{2}\right)} - l_{5} + \left(q_{3} + l_{2\min}\right)\cos(\alpha); \\ Y_{pc} &= \left(q_{2} - q_{1}\right)/2; Z_{pc} = \left(q_{3} + l_{2\min}\right)\sin(\alpha) + l_{4}\sin(\beta); \\ \beta &= \arctan2\left(Z_{pc}, X_{pc}\right); \alpha = \arccos\left(\frac{\left(A^{2} + B^{2} - l_{1}^{2} + C^{2}\right)}{\left(2\left(q_{3} + l_{2\min}\right) \cdot B\right)}\right); \\ A &= q_{3} + l_{2\min}; B = \sqrt{\left(4l_{3}^{2} - q_{1}^{2} + 2q_{2}q_{1} - q_{2}^{2}\right)/2 + l_{5}}; \\ C &= \left(q_{2} - q_{1}\right)/2. \end{split} \tag{4}$$

$$q_{1} = Y_{p} - \sqrt{\left(l_{1}^{2} - l_{4}^{2} - \left(X_{p}^{2} + Z_{p}^{2}\right) + 2l_{4}\sqrt{\left(X_{p}^{2} + Z_{p}^{2}\right)}\right)};$$

$$q_{2} = Y_{p} + \sqrt{\left(l_{1}^{2} - l_{4}^{2} - \left(X_{p}^{2} + Z_{p}^{2}\right) + 2l_{4}\sqrt{\left(X_{p}^{2} + Z_{p}^{2}\right)}\right)};$$

$$q_{3} = \left(N + \sqrt{D}\right) / \left(2r^{2}\right).$$
(5)

where:

$$\begin{split} N &= -2r^2 l_{2\min}; r^2 = X_p^2 + Z_p^2; D = T_1 + T_2 + T_3 + T_4 + T_5 + T_6; \\ T_1 &= 4Z_p^6 + 4X_p^6 + 12X_p^2 4Z_p^4; T_2 = 8X_p^5 l_5 + 16X_p^3 Z_p^2 l_5 + 8X_p Z_p^4 l_5; \\ T_3 &= 4r^2 (X_p^2 + Z_p^2) (l_3^2 + l_4^2 + l_5^2); \\ T_4 &= -r^2 \left(X_p^2 + Z_p^2\right) \left(q_1^2 + q_2^2\right) + 4r^2 q_1 q_2 - 2X_p^2 Z_p^2 \left(q_1^2 + q_2^2\right) + 4X_p^2 Z_p^2 q_1 q_2; \\ 4X_p^2 Z_p^2 q_1 q_2; \\ T_5 &= 4A \begin{bmatrix} X_p^5 + X_p^4 l_5 + 2X_p^3 Z_p^2 + 2X_p^2 Z_p^2 l_5 + X_p Z_p^4 + Z_{p5}^4 - \\ Br(X_p^3 + X_p Z_p^2) l_4 \end{bmatrix}; \\ T_6 &= -8Br l_4 \left[ X_p^3 + 2X_p^2 Z_p^2 + Z_p^4 + X_p^3 l_5 + X_p Z_p^2 l_5 \right]; \\ A &= \sqrt{\left(4l_3^2 - q_1^2 + 2q_2 q_1 - q_2^2\right)}; B = \sqrt{\left(X_p^2 + Z_p^2\right)}. \\ \begin{cases} \theta = \operatorname{atan} 2\left(\sin_\theta, \cos_\theta\right) \\ \psi = \operatorname{atan} 2\left(\sin_\theta, \cos_\theta\right) \end{cases} \end{split}$$
 (7)

where:

$$\begin{cases} \cos_{\theta} = \frac{\sqrt{(X_{RCM} - X_{P})^{2} + (Y_{RCM} - Y_{P})^{2} + (Z_{RCM} - Z_{P})^{2}}}{Z_{RCM} - Z_{P}} \\ \sin_{\theta} = \sqrt{1 - \cos_{\theta}^{2}} \end{cases}$$

$$\begin{cases} \sin_{\psi} = \frac{X_{RCM} - X_{P}}{\sqrt{(X_{RCM} - X_{P})^{2} + (Y_{RCM} - Y_{P})^{2} + (Z_{RCM} - Z_{P})^{2}}} \\ \frac{1}{\sin(\theta)} \end{cases}$$

$$\cos_{\psi} = \frac{Y_{RCM} - Y_{P}}{\sqrt{(X_{RCM} - X_{P})^{2} + (Y_{RCM} - Y_{P})^{2} + (Z_{RCM} - Z_{P})^{2}}} \cdot \frac{1}{\sin(\theta)} \end{cases}$$

$$(8)$$

Finally, the end-effector coordinates are:

$$\begin{cases} X_E = L \cdot \cos(\psi) \sin(\theta) + X_p \\ Y_E = L \cdot \sin(\psi) \sin(\theta) + Y_p \\ Z_E = L \cdot \cos(\theta) + Z_p \end{cases}$$
(9)

An innovative active instrument (Pisla, 2024 b) was developed and integrated with the robot.

The active instrument features a 10 mm diameter shaft with an articulated distal head and four degrees of freedom (DOF) to improve the workspace compared to standard rigid laparoscopic instruments,  $q_{insi}$ , i=1...4.

The 3D design of the instrument and the movements are illustrated in Figure 4.

Four actuators are used to control the instrument movements (Figure 4): opening/closing of the distal head  $(q_1)$ , rotation of the distal head  $(q_2)$ , flexible element bending  $(q_3)$  and the rotation of the entire rod  $(q_4)$ .

The flexible segment (Figure 4) provides distal head bending capability. The instrument is manufactured using 3D printing (Stratasys J5 Prime Med).

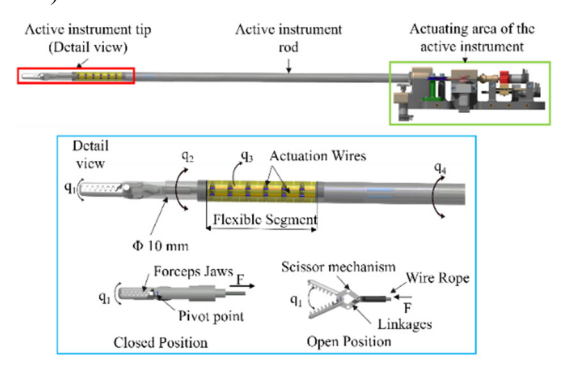


Figure 4: The 3D design of the active instrument and its movements.

### 3 THE CONTROL SYSTEM

The control system converts surgeon hand motions into robot commands using either a 3D Space Mouse (3DConnexion, Munich, Germany, 2001) or Omega.7 haptic device (Force Dimension, Switzerland, 2001) as master console. The robot reproduces the surgeon's movements following established safety measures (Vaida, 2016).

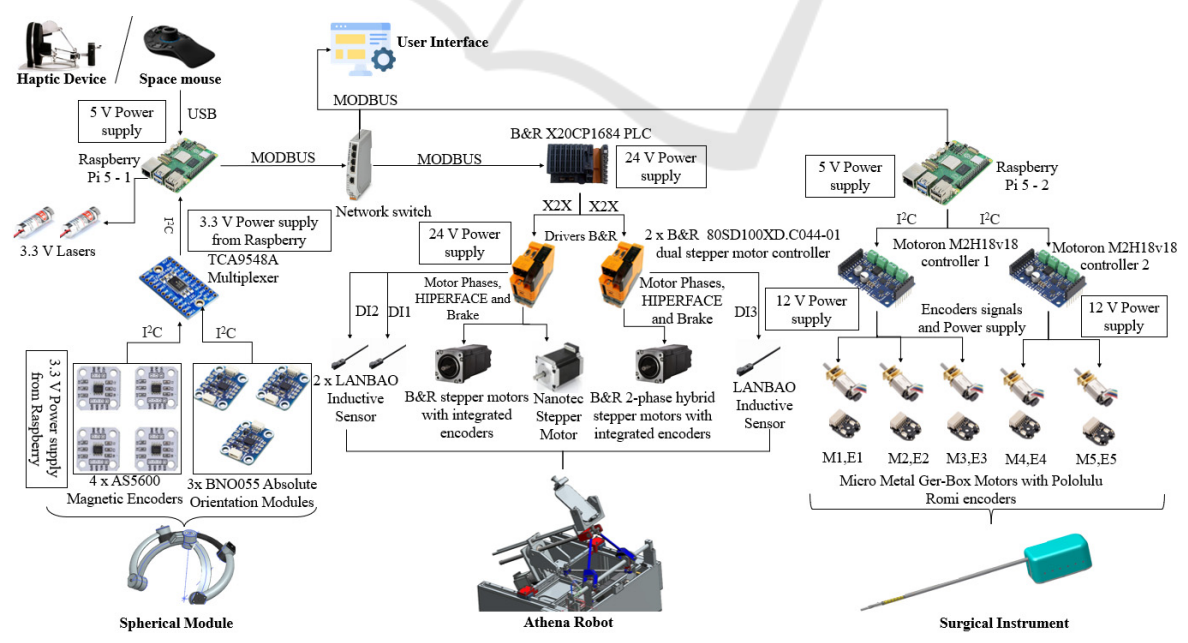


Figure 5: Hardware architecture of the Athena parallel robot.

Figure 5 illustrates the hardware architecture of the Athena parallel robot. The entire system can be divided into three main modules, the surgical instrument, the Athena robot and the spherical module.

To control the surgical instrument, five Pololu micro metal gear-box motors are used and to obtain position feedback five Pololu Romi encoders are used. To control the motors, two Motoron M2H18v18 controllers are used, with two different addresses. The controllers are receiving data that is converted to PWM signals from Raspberry Pi 5-2 via I<sup>2</sup>C BUS communication protocol that allows the Raspberry Pi to control multiple devices. The 12V supply powers the Motoron controllers and Pololu motors, while the 5V supply operates the Raspberry Pi 5-2.

The Athena robot is controlled using a B&R PLC system employing two B&R hybrid stepper motors and one Nanotec stepper motor with integrated encoders. Motor control is achieved using two B&R stepper controllers. Three LANBAO inductive sensors are used for the homing procedure.

To control both robot and the instrument, the Raspberry pi 5 - 1 is receiving the data from a 3D space mouse or from the haptic device via USB. The PLC is receiving data from the rasp Raspberry pi 5 – 1 via Modbus, being connected to the LAN network of the system though the Network Switch. The same protocol and LAN network is used to send data from the PLC to the second Raspberry Pi 5.

The spherical module represents the last element of the system. To know the position and the orientation of the module, three BNO055 Absolute orientation modules and four AS5600 magnetic encoders are used.

Three absolute orientation modules with 9-axis IMUs determine the spherical module's position and orientation.

Four magnetic encoders provide precise angle feedback for each revolute joint of the spherical mechanism. IMU sensors and encoders communicate with Raspberry Pi 5 via I<sup>2</sup>C protocol through a multiplexer powered by a 3.3 V supply. The multiplexer manages multiple I<sup>2</sup>C devices and prevents address conflicts, enabling simultaneous data acquisition from all sensors and encoders.

Two lasers powered from a 3.3 V supply are used to aid in the positioning of the RCM, with the RCM located at the intersection of both laser beams.

Figure 6 presents the state machines of the PLC and two raspberry PI 5 boards. On the PLC side, the initial state that is set on system power up is INIT, which waits for every component of the system to be powered up and ready for communication. If successful, the system proceeds to the IDLE state in which it awaits user inputs via the GUI such as: Homing, Power, Reset etc. Once the user selects the structure to control (Robot or active instrument) and a method of controlling said structure (Haptic or Space Mouse) the state machine switches to MOVE STATE. A secondary state machine allows the smooth change between controlling the robot and the active instrument and switching between control peripherals. The Auxiliary Raspberry PI 5 that is used for gathering data from the control peripherals and secondary sensors (BNO-055 and AS5600) is connected via MODBUS to the system's LAN network and presents a state machine of its own. A simple one that connects, reads and sends the data back to the PLC via Modbus. The instrument's Raspberry PI 5 also has a state machine that connects, reads commands and data from the PLC and moves the instrument's tip according to the user's input to grasp, bend, twist and rotate.

# 4 EXPERIMENTAL TESTING AND VALIDATION

Figure 7 illustrates the experimental setup that was developed. Robot calibration is required before testing (Pisla, 2009). The calibration consists of a homing procedure for the active linear joints of the robot  $(q_b, i=1...3)$ .

One IMU positioned on the robot frame represents the reference, the second is positioned on the link between the two spherical joints connecting the robot frame with the spherical mechanism and one on the spherical mechanism. The fixed one, positioned on the robot frame, is aligned with the robot reference system (*OXYZ*).

These sensors are only used once in the determination of the RCM, specifically at system power up, ensuring that angle drift has a minimal or no impact on the Euler angles.

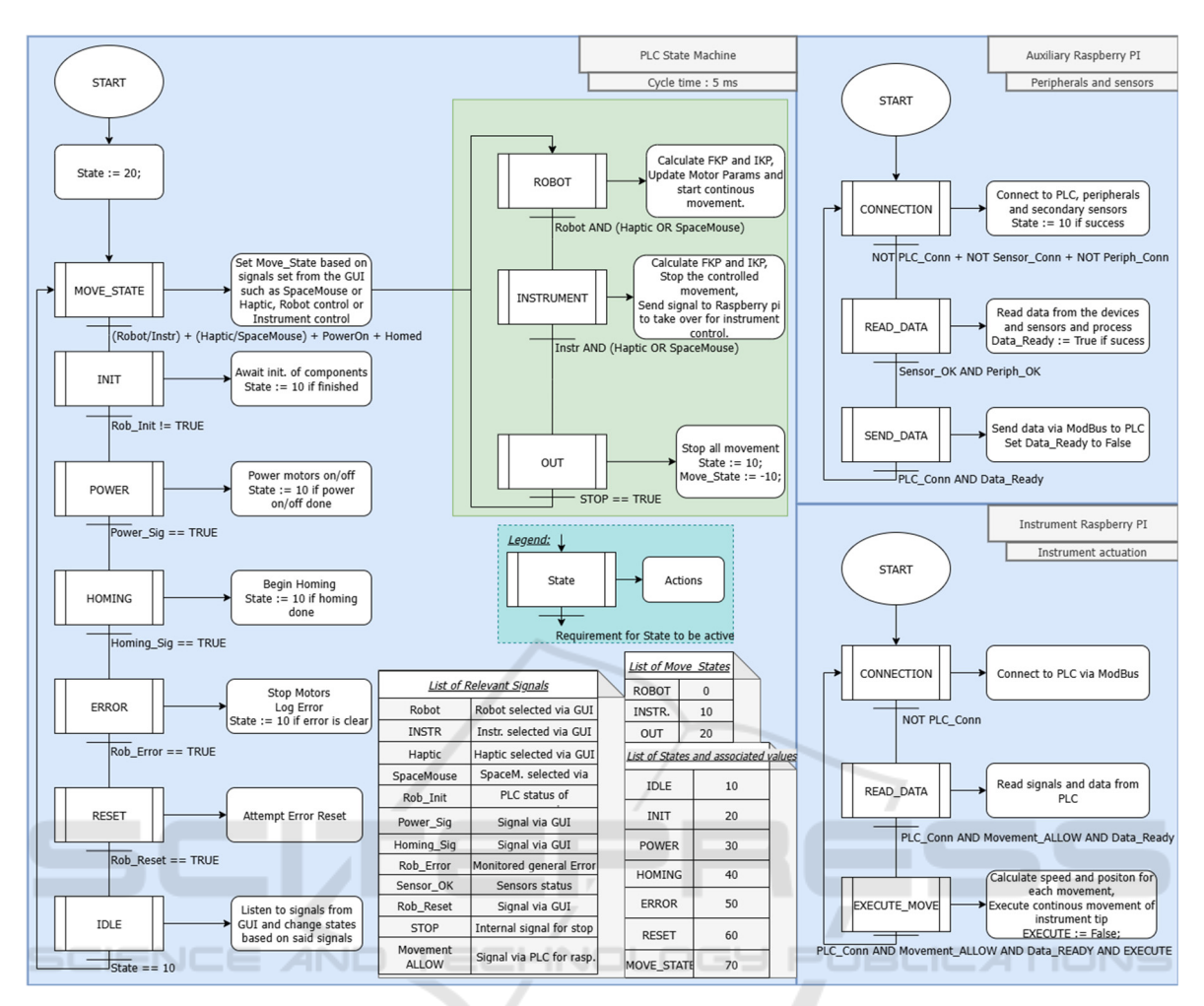


Figure 6: Athena parallel robot state machines.

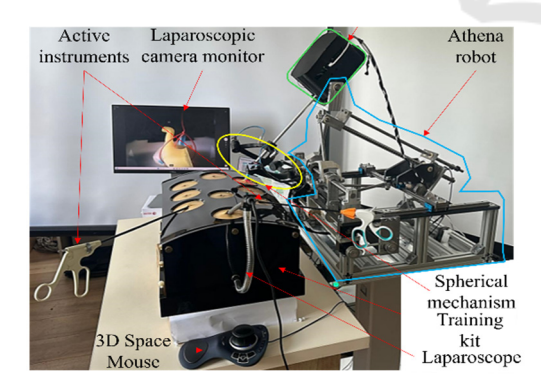


Figure 7: Experimental setup of the Athena robot.



Figure 8: Setup for RCM validation using Optitrack.

The RCM position within the robot coordinate frame is automatically calculated using the IMU sensors output, namely the yaw-pitch-roll angles (following the z-y-x rotation convention). Thus, the RCM position in the robot coordinates frame is:

$$\begin{bmatrix} X_{RCM}Y_{RCM}Z_{RCM}\mathbf{1} \end{bmatrix}^T = {}^{Sph1}_0 \begin{bmatrix} T \end{bmatrix} \cdot {}^{Sph2}_{Sph1} \begin{bmatrix} T \end{bmatrix} \cdot {}^{SphMec}_{Sph2} \begin{bmatrix} T \end{bmatrix} \cdot \begin{bmatrix} R001 \end{bmatrix}^T \tag{10}$$

where  ${}^{\text{Sphi}}_{0}[T]$  is the transformation matrix from the robot coordinate system to the first spherical joint,  ${}^{\text{Sphi}}_{\text{Sphi}}[T]$  the transformation matrix from the first to second spherical joint,  ${}^{\text{Sphi}}_{\text{Sphi}}[T]$  the transformation matrix from the second spherical joint to the passive spherical mechanism (the attaching point) and R is its radius (Vaida, 2025). Knowing the coordinates of point P (Eq. 3), the orientation of the instrument can be determined using Eqs. 7-9.

The OptiTrack measurement system was used to validate the detected RCM position obtained using

the IMU sensors and Eq 10. The setup for these measurements is illustrated in Figure 8, which shows the placement of the markers on the experimental model to determine the coordinate system axes and the actual position of the RCM (measured), as well as their display in the virtual environment using the Motive software program. The measurements were performed after the IMU sensors calibration, which reduces the drift) and the determined RMSE has been of 0.58 mm, with a maximum positioning error of 1.56 mm within the experimental tests.

Experimental tests were performed using a minimally invasive surgery kit (Figure 9) with 3D printed pancreas and stomach. The soft-material organs (Vaida, 2025) enable testing scenarios where the instrument grasps and withdraws the stomach from the pancreatic field, holding it outside the intraoperative workspace required for pancreatic procedures.

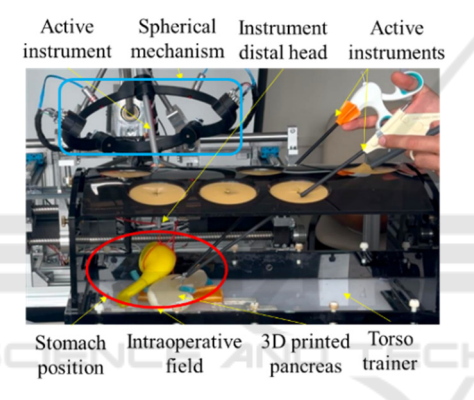


Figure 9: Stomach grasping and manipulation to generate intraoperative field.

## 5 CONCLUSIONS

This paper presents the control architecture for the Athena robot, a surgical assistant for laparoscopic pancreatic surgery that manipulates an active instrument. The master-slave control system uses either a 3D Space Mouse or haptic device (Omega.7) as the master console. The architecture integrates hardware and software components to enable precise surgical manipulation. Surgeons can define the RCM position before insertion and modify it during surgery as required. OptiTrack Motion Capture system validation confirmed the approach's accuracy. Experimental tests used a minimally invasive surgery kit with 3D printed pancreas and stomach to demonstrate the flexibility and dexterity for pancreatic surgery. Future research will focus on experimental tests to simulate resection and

reconstruction of the pancreas during the Whipple procedure, using a pancreas realized at a scale of 1 to 1 based on 3D reconstruction using real CT scan data, improvement of the GUI and integration of the robot into a surgical simulator.

#### **ACKNOWLEDGEMENTS**

This research was funded by the project New smart and adaptive robotics solutions for personalized minimally invasive surgery in cancer treatment - ATHENA, funded by European Union – Next Generation EU and Romanian Government, under National Recovery and Resilience Plan for Romania, contract no. 760072/23.05.2023, code CF 116/15.11.2022, through the Romanian Ministry of Research, Innovation and Digitalization, within Component 9, investment 18.

#### REFERENCES

McGuigan, A., Kelly, P., Turkington, R. C., Jones, C., Coleman, H. G., McCain, R. S. Pancreatic cancer: A review of clinical diagnosis, epidemiology, treatment and outcomes. W. J. of Gastroenterology, 24(43),4846–4861, 2018. doi:10.3748/wjg.v24.i43.4846.

Asbun, D., Lluis, N., Jimenez, R.E., Asbun, H. J. A narrative review of minimally invasive pancreatic surgery: from pipedreams to pancreatoduodenectomies, DMR 7(0), DMR9393, 2023.

Balzano, G., Zerbi, A., Aleotti, F., Capretti, G., Melzi, R., Pecorelli, N. et al. Total Pancreatectomy With Islet Autotransplan-tation as an Alternative to High-risk Pancreatojejunostomy After Pancreaticoduodenectomy: A Prospective Randomized Trial. Annals of Surgery 277(6): p894-903, 2023. doi: 10.1097/SLA.00000000000005713.

Bergholz, M., Ferle, M. & Weber, B.M. The benefits of haptic feedback in robot assisted surgery and their moderators: a meta-analysis. Sci Rep 13, 19215, 2023. doi: 10.1038/s41598-023-46641-8.

Cawich, S. O., Cabral, R., Douglas, J., Thomas, D. A., Mohammed, F. Z., Naraynsingh, V., & Pearce, N. W. Whipple's procedure for pancreatic cancer: training and the hospital environment are more important than volume alone. Surgery in Practice and Science, 14, 100211, 2023. doi: 10.1016/j.sipas.2023.100211.

Damoli, I., Butturini, G., Ramera, M., Paiella, S., Marchegiani, G., Bassi, C. Minimally invasive pancreatic surgery - a review. Wideochir Inne Tech Maloinwazyjne; 10(2):141-149; 2015. doi:10.5114/wiitm.2015.52705.

De Pastena, M., van Bodegraven, E. A., Mungroop, T. H., Vissers, F. L., Jones, L. R., Marchegiani, G. et al. Distal pancreatectomy fistula risk score (D-FRS):

- development and international validation. Annals of Surgery, 277(5), e1099-e1105, 2023. doi: 10.1097/SLA.00000000000005497.
- Rus, G., Andras, I., Vaida, C., Crisan, N., Gherman, B., Radu, C., Tucan, P., Iakab, S., Hajjar, N.A., & Pisla, D. Artificial Intelligence-Based Hazard Detection in Robotic-Assisted Single-Incision Oncologic Surgery. Cancers, 15, 3387, 2023. doi: 10.3390/cancers15133387.
- Haidegger, T., Speidel, S., Stoyanov, D., & Satava, R. M. Robot-assisted minimally invasive surgery—Surgical robotics in the data age. Proceedings of the IEEE, 110(7), 835-846, 2022. doi: 10.1109/JPROC.2022.3180350.
- Kastelan, Z., Hudolin, T., Kulis, T., Knezevic, N., Penezic, L., Maric, M., & Zekulic, T. Upper urinary tract surgery and radical prostatectomy with Senhance® robotic system: Single center experience—First 100 cases. The International Journal of Medical Robotics and Computer Assisted Surgery, 17(4), e2269, 2021. doi: doi.org/10.1002/rcs.2269.
- Khachfe, H.H., Habib, J.R., Harthi, S.A. et al. Robotic pancreas surgery: an overview of history and update on technique, outcomes, and financials. J Robotic Surg 16, 483–494, 2022. doi:10.1007/s11701-021-01289-2.
- Korayem, M. H., & Vahidifar, V. (2022). Detecting hand's tremor using leap motion controller in guiding surgical robot arms and laparoscopic scissors. Measurement, 204. 112133. (a)
- Korayem, M. H., Madihi, M. A., & Vahidifar, V. (2021). Controlling surgical robot arm using leap motion controller with Kalman filter. Measurement, 178, 109372.
- Korayem, M. H., Vosoughi, R., & Vahidifar, V. (2022). Design, manufacture, and control of a laparoscopic robot via Leap Motion sensors. Measurement, 205, 112186. (b)
- Li, J., et al (2023). Application of Improved Robot-assisted Laparoscopic Telesurgery with 5G Technology in Urology. European urology, 83(1), 41–44. doi: 10.1016/j.eururo.2022.06.018.
- McGuigan, A., Kelly, P., Turkington, R. C., Jones, C., Coleman, H. G.,McCain, R. S. Pancreatic cancer: A review of clinical diagnosis, epidemiology, treatment and outcomes. W. J. of Gastroenterology, 24(43),4846– 4861, 2018. doi:10.3748/wjg.v24.i43.4846.
- Melvin WS, Needleman BJ, Krause KR, Ellison EC. Robotic resection of pancreatic neuroendocrine tumor. J Laparoendosc Adv Surg Tech A.; 13:33–6, 2003. doi: 10.1089/109264203321235449.
- Minamimura, K., Aoki, Y., Kaneya, Y., Matsumoto, S., Arai, H., Kakinuma, D., & Yoshida, H. Current status of robotic hepatobiliary and pancreatic surgery. Journal of Nippon Medical School, 91(1), 10-19, 2024.
- Najafinejad, A., & Korayem, M. H. (2023). Detection and minimizing the error caused by hand tremors using a leap motion sensor in operating a surgeon robot. Measurement, 221, 113544.
- Nießen, A, Hackert, T. State-of-the-art surgery for pancreatic cancer. Langenbecks Arch Surg.;407(2):443-450, 2022.
- Nortunen, M., Meriläinen, S., Ylimartimo, A., Peroja, P., Karjula, H., Niemelä, J., Saarela, A., Huhta, H.

- Evolution of pancreatic surgery over time and effects of centralizationa single-center retrospective cohort study. J Gastrointest Oncol. 2023;14(1):366-378. doi:10.21037/jgo-22-649.
- Pisla, D., Carami, D., Gherman, B., Soleti, G., Ulinici, I., Vaida, C. A novel control architecture for roboticassisted single incision laparoscopic surgery. The Romanian Journal of Technical Sciences. Applied Mechanics., 66(2), 141-162, 2021.
- Pisla, D., Popa, C., Pusca, A., Ciocan, A., Gherman, B.,
  Mois, E., Cailean, A.-D., Vaida, C., Radu, C., Chablat,
  D., Al Hajjar, N. On the Control and Validation of the
  PARA-SILSROB Surgical Parallel Robot. Appl. Sci.,
  14, 7925, 2024. doi: 10.3390/app14177925. (a)
- Pisla, D., Chablat, D., Birlescu, I., Vaida, C., Pusca, A., Tucan, P. Gherman, B. AUTOMATIC INSTRUMENT FOR ROBOT-ASSISTED MINIMALLY INVASIVE SURGERY. Romania, Patent number: RO138293A0. 2024, pp.15. (b)
- Pisla, D., Plitea, N., Gherman, B., Pisla, A., Vaida, C.
  Kinematical Analysis and Design of a New Surgical
  Parallel Robot. In Computational Kinematics;
  Kecskeméthy, A., Müller, A., Eds.; Springer:
  Berlin/Heidelberg, Germany, 2009.
- Tucan, P., Vaida, C., Horvath, D., Caprariu, A., Burz, A., Gherman, B., Iakab, S., Pisla, D. Design and Experimental Setup of a Robotic Medica Instrument for Brachytherapy in Non-Resectable Liver Tumors. Cancers, 2022, 14, 5841.
- Tucan, P.; Ciocan, A.; Gherman, B.; Radu, C.; Vaida, C.;
  Hajjar, N.A.; Chablat, D.; Pisla, D. Design
  Optimization of a Parallel Robot for Laparoscopic
  Pancreatic Surgery Using a Genetic Algorithm. Appl.
  Sci., 15, 4383., 2025. doi:10.3390/app15084383.
- Vaida, C., Ciocan, A., Caprariu, A., Radu, C., Al Hajjar, N., Pisla, D. A 3D-printed anatomical pancreas model for Robotic assisted Minimally Invasive Surgery. Journal of Functional Biomaterials. J. Funct. Biomater. 2025, 16, 207. (a)
- Vaida, C.; Birlescu, I.; Gherman, B.; Condurache, D.; Chablat, D.; Pisla, D. An analysis of higher-order kinematics formalisms for an innovative surgical parallel robot. Mech. Mach. Theory, 2025, 209, 105986. (b)
- Vaida, C.; Pisla, D.; Schadlbauer, J.; Husty, M.; Plitea, N. Kinematic analysis of an innovative medical parallel robot using study parameters. In New Trends in Medical and Service Robots. Mechanisms and Machine Science; Wenger, P., Chevallereau, C., Pisla, D., Bleuler, H., Rodić, A., Eds.; Springer: Cham, Switzerland, 2016; Volume 39.
- Wong MCS, Jiang JY, Liang M, Fang Y, Yeung MS, Sung JJY. Global temporal patterns of pancreatic cancer and association with socioeconomic development. Sci Rep. 2017;7(1):3165. Published 2017 Jun 9. doi:10.1038/s41598-017-02997-2.
- Zhang, W., Wang, Z., Ma, K. et al. State of the art in movement around a remote point: a review of remote center of motion in robotics. Front. Mech. Eng. 19, 14 2024. doi:10.1007/s11465-024-0785-3.